Journal of Cancer Research and Clinical Oncology (2025) 151:104
https://doi.org/10.1007/s00432-025-06146-5

RESEARCH

Identification of LIMK1 as a biomarker in clear cell renal cell carcinoma: from data mining to validation

Yifei Li[1] · Congcong Fan[1] · Feng Jiang[1] · Jingnan Zhang[1] · Yanzhen Li[1] · Yanjie Jiang[1] · Rui Zhang[1] · Zhixian Yu[2] · Siqi Wang[2]

Received: 24 October 2024 / Accepted: 20 February 2025 / Published online: 8 March 2025

Abstract

Purpose Clear cell renal cell carcinoma (ccRCC) is one of the most common types of renal cancer. LIM kinase 1 (LIMK1) reportedly plays an important role in tumorigenesis. However, the involvement of LIMK1 in the progression of ccRCC remains ambiguous.

Methods Based on the TCGA and CPTAC databases, the expression of LIMK1 in ccRCC was evaluated. In the TCGA-ccRCC cohort, the relationships between LIMK1 and immune cell infiltration as well as immune checkpoints were assessed. The high expression of LIMK1 in ccRCC was verified by qRT-PCR in four RCC cell lines. Immunohistochemistry was used to evaluate the expression of LIMK1 in clinical samples. The association between LIMK1 expression and survival prognosis was explored via Kaplan-Meier survival curve in the TCGA-ccRCC and local cohorts. The effects of LIMK1 knockdown on the proliferation, migration, and invasion abilities of RCC cells were evaluated via colony, CCK-8, wound healing, and Transwell assays.

Results Elevated expression level of LIMK1 was found in the TCGA-ccRCC cohort and was confirmed in RCC cell lines and clinical samples. Up-regulation of LIMK1 was found to be correlated with poor prognosis in TCGA-ccRCC and external cohorts. In addition, high-LIMK1 was associated with clinicopathological stage, immune cell infiltration and immune checkpoint in ccRCC. Importantly, knockdown of LIMK1 diminished the capability of proliferation, migration, and invasion in RCC cells.

Conclusion LIMK1 may serve as a promising diagnostic and prognostic biomarker of ccRCC.

Keywords Clear cell renal cell carcinoma · LIMK1 · Immunity · Diagnosis · Prognosis

Abbreviations

ccRCC	Clear cell renal cell carcinoma
LIMK1	LIM kinase 1
TCGA	The Cancer Genome Atlas
CPTAC	The Cancer Proteomic Tumor Analysis Consortium
TSGs	Tumor suppressor genes
APC	Adenomatous polyposis coli
PTEN	Phosphatase and tensin homologue
DEGs	Differential expression genes
THPA	The Human Protein Atlas
DCs	Dendritic cells
KEGG	Kyoto Encyclopedia of Genes and Genomes
GO	Gene Ontology
OS	Overall survival
HR	Hazard ratio

Yifei Li and Congcong Fan contributed equally to this work.

✉ Siqi Wang
wangsiqi@wmu.edu.cn

[1] Zhejiang Key Laboratory of Intelligent Cancer Biomarker Discovery and Translation, The First Affiliated Hospital of Wenzhou Medical University, Wenzhou 325000, China

[2] Department of Urology, The First Affiliated Hospital of Wenzhou Medical University, Wenzhou, China

Introduction

Based on the latest cancer statistics reported by the World Cancer Organization, the global incidence of renal cancer is ~431,288 new cases (2.2% of all cancer cases), and 179,368 deaths (1.8% of total cancer-related deaths) (Sung

et al. 2021). The most common malignant renal cancer is renal cell carcinoma (RCC) (Jemal et al. 2011). It can be divided into different subtypes, including clear cell RCC (ccRCC), papillary RCC, and chromophobe RCC (Moch et al. 2016). Among these, ccRCC is the most common subtype, accounting for 75–80% of all RCCs, and contributed to 2.3% of global cancer deaths in 2022 (Hsieh et al. 2017; Zhang et al. 2022). Moreover, metastases are common in patients with ccRCC, resulting in poor prognosis and unsatisfied treatment efficiency (Jonasch et al. 2021). Despite the improvement in survival rates for early-stage ccRCC using current treatment methods, such as radical or partial nephrectomy, managing advanced ccRCC remains a challenge (Ljungberg et al. 2015). Notably, ccRCC is highly resistant to conventional anti-cancer treatment, including radio- and cytotoxic chemotherapy (Cohen and McGovern 2005; Hammers 2016). Thus, defining the mechanisms driving ccRCC development and identifying potential therapeutic targets are urgently needed for patients with ccRCC.

LIM kinase 1 (LIMK1), also known as LIMMK1, is a member of the LIM motif-containing protein kinase family, which regulates actin cytoskeleton dynamics through the phosphorylation of cofilin (Bénédetti and Vallée 2023; Scott and Olson 2007). In recent years, LIMK1 has received extensive attention for its involvement in cell proliferation, cell migration, and tumorigenesis (Scott and Olson 2007; Villalonga et al. 2023; McConnell et al. 2011). Moreover, abnormal activation of LIMK1 has been identified in several cancer types, including breast, prostate, and colorectal cancers (Gong et al. 2019; Fu et al. 2018; Zhang et al. 2018). Yet, it is not clear whether LIMK1 plays a role in ccRCC progression.

In this study, multiple bioinformatic analyses based on the Cancer Genome Atlas (TCGA) and the Cancer Proteomic Tumor Analysis Consortium (CPTAC) databases revealed the up-regulation of LIMK1 in ccRCC tissues at both the mRNA and protein levels. It was found that there was a negative correlation between LIMK1 and tumor suppressor genes (TSGs) (adenomatous polyposis coli (APC) and phosphatase and tensin homologue (PTEN)). LIMK1 was correlated with immune cell infiltration landscape and expressions of immune checkpoint genes. Moreover, reduced LIMK1 impedes proliferation, migration, and invasion of RCC cells (A-498 cells and 786-0 cells). LIMK1 may enhance drug sensitivity of compounds, such as Bleomycin, Simvastatin, Everolimus, Staurosporine, Rapamycin and Wortmannin. Collectively, these results suggest the oncogenic role of LIMK1 within ccRCC.

Materials & methods

Exploration of LIMK1 mRNA level

The genomics data matrix of TCGA, containing LIMK1 expression files across 23 different cancer types, including the TCGA-ccRCC cohort, was obtained from the UCSC Xena website. Notably, both clinical information and genomics matrix files specific to the TCGA-ccRCC cohort were selected for analysis. Differential expression genes (DEGs) between the high- and low-LIMK1 expression groups, based on median LIMK1 expression, were determined using the R package 'DESeq2' with an adjusted p-value of 0.05 and a$|\log_2$-fold change$| > 1.5$.

Examining LIMK1 protein level

CPTAC-ccRCC proteomics data, which included 110 tumor samples and 84 normal adjacent tissue samples, were acquired from the CPTAC platform. The LIMK1 protein level in ccRCC tissues was labeled with isobaric mass tags for quantification with Tandem Mass Tags according to a previously published protocol (Mertins et al. 2018). The localization of LIMK1 in three cell lines (U-251MG, U2OS, and A-431) was derived from The Human Protein Atlas (THPA) database which was utilized to measure the LIMK1 protein level in ccRCC tissues. Antibody HPA073571 and Antibody HPA028516 were used.

DNA methylation analysis

The methylation analysis of LIMK1 in ccRCC samples was conducted using the SMART software (Li et al. 2019). Based on the TCGA data, comprehensive DNA methylation analysis and visualization plots were generated. The SMART software provided a summarized overview, offering insights into the distribution and chromosomal positioning of methylation probes pertaining to the gene of interest. The comparison of methylation level of each site between ccRCC and normal tissues was performed using Wilcoxon test. The data from MethSurv database was used to identify the effect of methylation level of specific sites on the survival probability of patients with ccRCC (Yu et al. 2021).

Immune-related characteristics analysis

The relevance between LIMK1 expression and TSGs was analyzed using the Spearman correlation analysis in R software. The R package 'ggplot' was used for visualization. With the TIMER database, the correlation between survival and LIMK1 expression was evaluated, as well as immune cell infiltration in patients with ccRCC. The correlations

between LIMK1 expression and immune purity, T cells, B cells, macrophages, neutrophils, and dendritic cells (DCs) were analyzed via spearman correlation analysis.

Analysis of affected signaling pathways and functional enrichment

The potential pro-oncogenic signaling pathways were included in the analysis based on the UALCAN platform and CPTAC database. For insights into the Kyoto Encyclopedia of Genes and Genomes (KEGG) pathways and Gene Ontology (GO), the KEGG REST API and R package 'org.Hs.eg.db' were used to clarify gene annotations. Enrichment analysis was performed via the R package 'clusterProfiler'. The minimum and maximum gene set was respectively 5 and 5,000. Statistical significance thresholds were set at $p < 0.05$ and a false discovery rate < 0.1.

Survival analysis and relevance of clinicopathologic features

The samples from the First Affiliated Hospital of Wenzhou Medical University (FAHWMU) cohort ($n = 120$) were collected to validate the prognostic value of LIMK1. Clinical parameters of patients in FAHWMU cohort were shown in Table S1. The association between LIMK1 expression and overall survival (OS) of patients with ccRCC was detected using the R package 'survival'. Univariate and multivariate Cox regression analyses was conducted via the R package 'Forest Plot'. Metrics included a 95% confidence interval, the hazard ratio (HR), and the log-rank p-value calculated by logistic regression analysis.

Differential analysis of mutation genes

A total of 366 samples with mutation data were downloaded from TCGA. The chi-square test was used to assess the difference in mutation frequency in each group of samples.

Cell culture and quantitative real-time PCR (qRT-PCR)

The HK-2 cell line, ACHN cell line, and A-498 cell line were cultured in MEM medium. 786-0 cells and caki-1 cells were cultured in RPMI-1640 medium and McCoy's 5 A medium, respectively. Cell lines were cultivated in mediums supplemented with 10% fetal bovine serum, and incubated at 37 °C with 5% CO_2. All cell lines were purchased from Wuhan Sevier Biotechnology Company. For total mRNA extraction, TRIzol Reagents were employed. To perform reverse transcription, the Revert Aid First Strand cDNA Synthesis Kit (Thermo Fisher Scientific, Waltham, MA, USA) was employed. For qRT-PCR, the 7500 Fast Real-Time PCR System was performed with SYBR Green Master Mix. GAPDH served as a control for comparison. The $2^{-\Delta\Delta Ct}$ method was used to calculate the relative levels of mRNA. The primer sequences of LIMK1 and GAPDH are shown in Table S2.

Western blotting

Cells were lysed with RIPA buffer, supplemented with a protease inhibitor cocktail. Protein concentrations were measured using a BCA Protein Assay Kit. Protein samples were separated by 10% SDS-PAGE gels and transferred onto PVDF membranes. After blocking, the membranes were incubated with primary antibodies overnight at 4 °C. The membranes were then washed and incubated with secondary antibodies. The visualization and quantification of protein bands were conducted through chemiluminescence detection system and ImageJ software, respectively. GAPDH was used as the internal control.

Transfection

Small interfering RNAs (si-LIMK1#1/2/3) were synthesized by GenePharma (Suzhou, China). Cells were seeded (8×10^4 cells/well) in 6-well plates and incubated at 37 °C with 5% CO_2. As per manufacturer instructions, A-498 and 786-0 cells were transfected with si-LIMK1 to knockdown the expression of LIMK1. The sequences of si-LIMK1#1/2/3 were shown in Table S3.

Cell proliferation, migration, and invasion assay

Following adequate digestion, the LIMK1-knockdown A-498 cells were placed in 96-well culture plates at a concentration of 4×10^3 cells/well and then maintained at 37 °C with 5% CO_2. The CCK-8 kit was utilized to assess absorbance at 450 nm daily for three days. For migration and invasion assays, A-498 cells with or without si-LIMK1 were inoculated in transwell chambers. A total of 3×10^4 cells/well were seeded onto the transwell upper chamber. The lower chamber was filled with a culture medium containing 10% FBS. Cells were incubated for 24 h at 37 °C and 5% CO_2. Following the manufacturer's instruction, formaldehyde fixation and 0.5% crystal violet staining of the transwell chambers were carried out. For 786-0 cells, colony assay, transwell assay and wound healing assay were performed after LIMK1 knockdown. Briefly, for the colony assay, a total of 1×10^3 cells per well were seeded in 6-well plates, following RNA transfection for 48 h. Subsequently, after an incubation period of 6 days, cells were stained to visualization and

counting. For the wound healing assay, cells were seeded in 6-well plates 48 h after RNA transfection. Upon reaching 95-100% confluency, a scratch was created using a 1000 µl pipette tip. Images were acquired using microscopy at 0 h and 24 h.

Drug sensitivity analysis

CellMiner is a database of anti-tumor drugs for 60 cell lines (9 cancers). The 263 drugs included are FDA approved drugs or clinical trial drugs. The sensitivity correlation between LIMK1 and anti-tumor drugs was completed by pearson correlation analysis via R packages 'impute', 'limma', 'ggplot2' and 'ggpubr'.

Immunohistochemistry (IHC)

Following fixation in 4% formalin and blocking, tumor tissue sections were subjected to overnight incubation at 4 °C with primary antibodies. Hematoxylin was utilized for nuclei counterstaining, while DAB kits were employed for visualization. Microscopic images were captured using a Leica DM4B microscope.

Statistical analysis

The Kruskal-Wallis test was used to assess the gene expression in different tumor tissues. The Wilcoxon rank-sum test was used to compare gene expression between normal and tumor tissues. Unpaired two-tailed Student's t-test was used for comparison between two groups and one-way analysis of variance between multiple groups. All statistical analyses were conducted using R software or GraphPad Prism, with significance set at the following parameters: $*p<0.05$, $**p<0.01$, $***p<0.001$.

Results

Upregulation of LIMK1 in CcRCC

To determine whether LIMK1 is dysregulated in cancers, the mRNA levels of LIMK1 were examined across 23 cancer types. Upregulation of LIMK1 was found in 21 out of 23 cancer types (Fig. 1A). Furthermore, analysis of the TCGA-ccRCC cohort data unveiled a significant upregulation of LIMK1 at the mRNA level in ccRCC (Fig. 1B). Also, higher LIMK1 protein levels were showed in ccRCC tissues (Fig. 1C). In line with it, compared to the normal kidney cells (i.e., HK-2), high expression of LIMK1 was validated in four RCC cell lines (ACHN, A-498, 786-0, and caki-1) (Fig. 1D). Based on the THPA database, IHC analysis of LIMK1 confirmed enhanced LIMK1 expression in most ccRCC samples. Two antibodies (HPA073571 and HPA028516) were used. For HPA073571, 12 cases showed strong intensity. For HPA028516, 1 case showed strong intensity, 8 cases showed moderate intensity, and 3 cases showed weak intensity (Fig. 2A and Figure S1A). Moreover, in the FAHWMU cohort, the expression of LIMK1 protein was stronger in ccRCC tissues compared to adjacent non-tumor tissues (Figure S2). As depicted in Fig. 2B, LIMK1 was predominantly observed in the cytosol and nuclear speckles. Individual fluorescent images of the three components were shown in Figure S1B.

DNA methylation of LIMK1 in patients with CcRCC

It has been reported that DNA methylation plays a vital role in the regulation of gene expression (Zhou et al. 2022). Based on the TCGA data, it was revealed that methylation levels of LIMK1 were reduced in most cancer types, including ccRCC (Fig. 3A). To examine whether LIMK1 is associated with its methylation, the DNA methylation level of LIMK1 was analyzed in patients with ccRCC. Clearly, there were 14 LIMK1 methylation sites in chromosome 12 (Fig. 3B). In brief, five sites are situated within the Island region (cg07594845, cg05640558, cg03358373, cg21437766, cg27651035), three sites are located in the N_Shore region (cg05592398, cg06126335, cg06757357), and the remaining six sites (cg22228754, cg03841431, cg25333521, cg00334821, cg06733155, cg04663932) are situated in gene body region. Analysis of methylation levels at the methylation sites revealed that LIMK1 was hypomethylated in ccRCC tissues compared with normal tissues, which potentially leads to high LIMK1 expression (Fig. 3C). Further, the association between methylation level of each site and survival probability was investigated. Multiple methylation sites associated with prognosis were identified, including cg05640558, cg04663932, cg00334821, cg25333529, cg22228754, cg03358373, and cg07594845 (Figure S3).

LIMK1 expression was associated with the clinicopathologic parameters

Clinicopathological factors indicate both the advancement of cancer and the efficiency of treatment (Pavlović and Heindryckx 2021). Whether LIMK1 expression is correlated with clinical characteristics (including age, histological grade score, pathological stage, and TNM scores) was analyzed in the TCGA-ccRCC cohort. As depicted in Fig. 4A-F, elevated LIMK1 expression was found in ccRCC patients with high histological grade, severe pathological stage, and high TNM scores. Kaplan-Meier

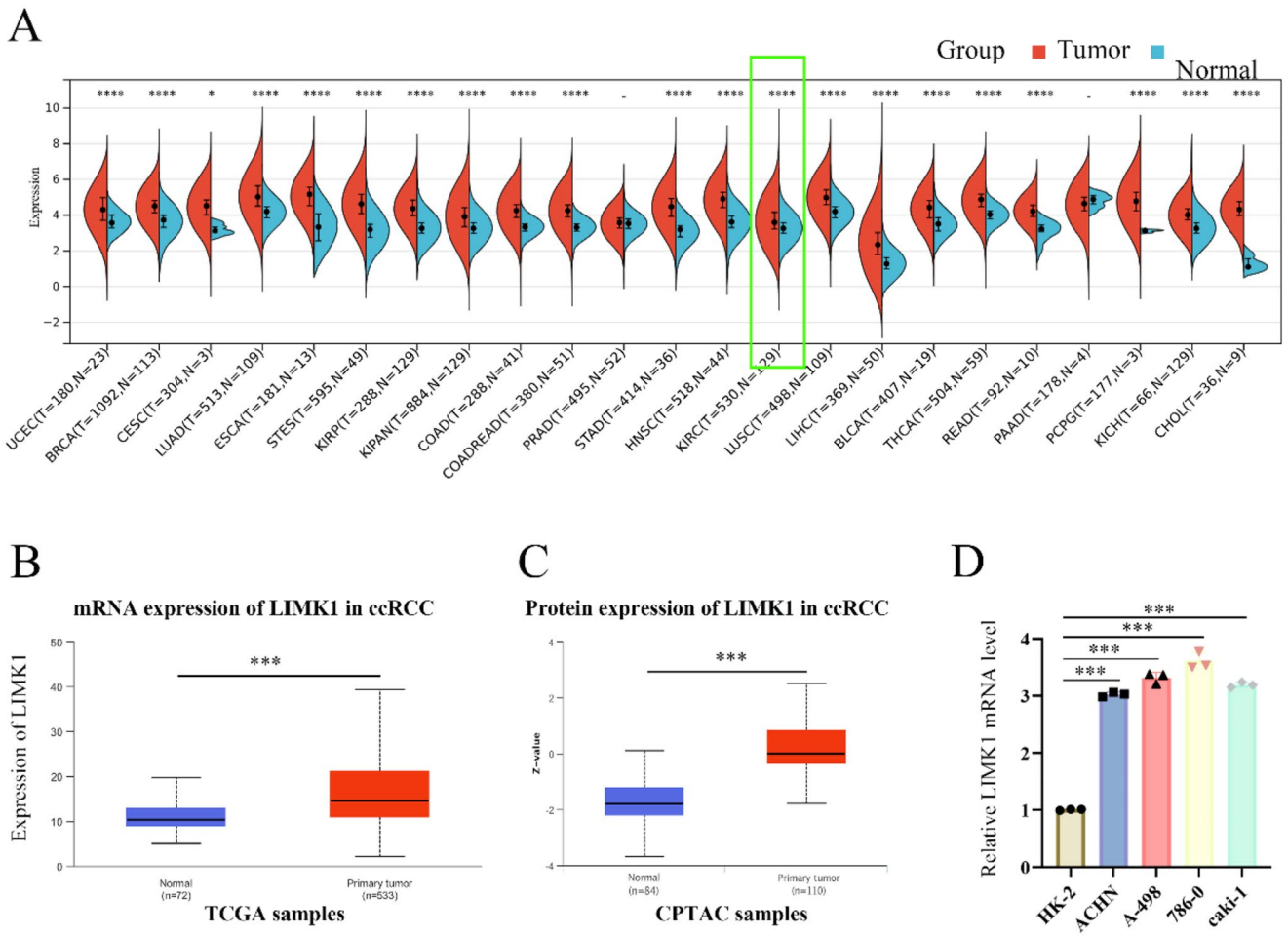

Fig. 1 Upregulation of LIMK1 in ccRCC. (**A**) Analysis of LIMK1 in 23 TCGA cancers, containing ccRCC. Red represents tumor samples and blue is for normal samples. Analyzing the LIMK1 expression in (**B**) TCGA-ccRCC cohort and (**C**) CPTAC dataset. (**D**) Validation of high expression of LIMK1 in RCC cell lines (ACHN, A-498, 786-0, and caki-1). *$p<0.05$, ***$p<0.001$, ****$p<0.0001$, n.s. $p>0.05$

survival analysis showed that elevated LIMK1 expression was correlated with unfavorable prognosis in TCGA-ccRCC and FAHWMU cohorts (Fig. 4G and Figure S4A). Receiver operating characteristic (ROC) curve analysis indicated that LIMK1 expression exhibited a great diagnostic performance in ccRCC (area under the curve (AUC) value = 0.75) (Fig. 4H). Meanwhile, the AUC values in FAHWMU cohort also demonstrated the accuracy of the LIMK1 in predicting the prognosis of ccRCC patients (Figure S4B). Univariate and multivariate Cox analysis showed that LIMK1 was an independent predictor (Figure S5). As shown in Figure S6, LIMK1 was found to be related to the BAP1 mutation, which has been reported to be involved in ccRCC development (Bi et al. 2016; Joseph et al. 2016). These results suggest that LIMK1 may play a role in the progression of ccRCC and exhibit promising prognostic value of ccRCC.

Involvement of signaling pathways and functional enrichment

Next, we explored the potential affected signaling pathways associated with LIMK1 protein level in ccRCC. These pathways encompassed chromatin modifier alteration, Hippo, mTOR, MYC/MYCN, NRF2, p53/Rb, RTK, SWI-SNF complex, and WNT. Remarkably, the above signaling pathways exhibited a strong variation when LIMK1 protein levels were changed (Fig. 5A–I). DEGs, obtained from the comparison of high- and low-LIMK1 groups, were used for GO and KEGG analyses. GO analysis showed the enrichment in axon development, actin cytoskeleton, and mitochondrial matrix (Fig. 5J). KEGG analysis revealed that the MAPK signaling pathway, Ras signaling pathway, and regulation of the actin cytoskeleton pathway were enriched (Fig. 5K).

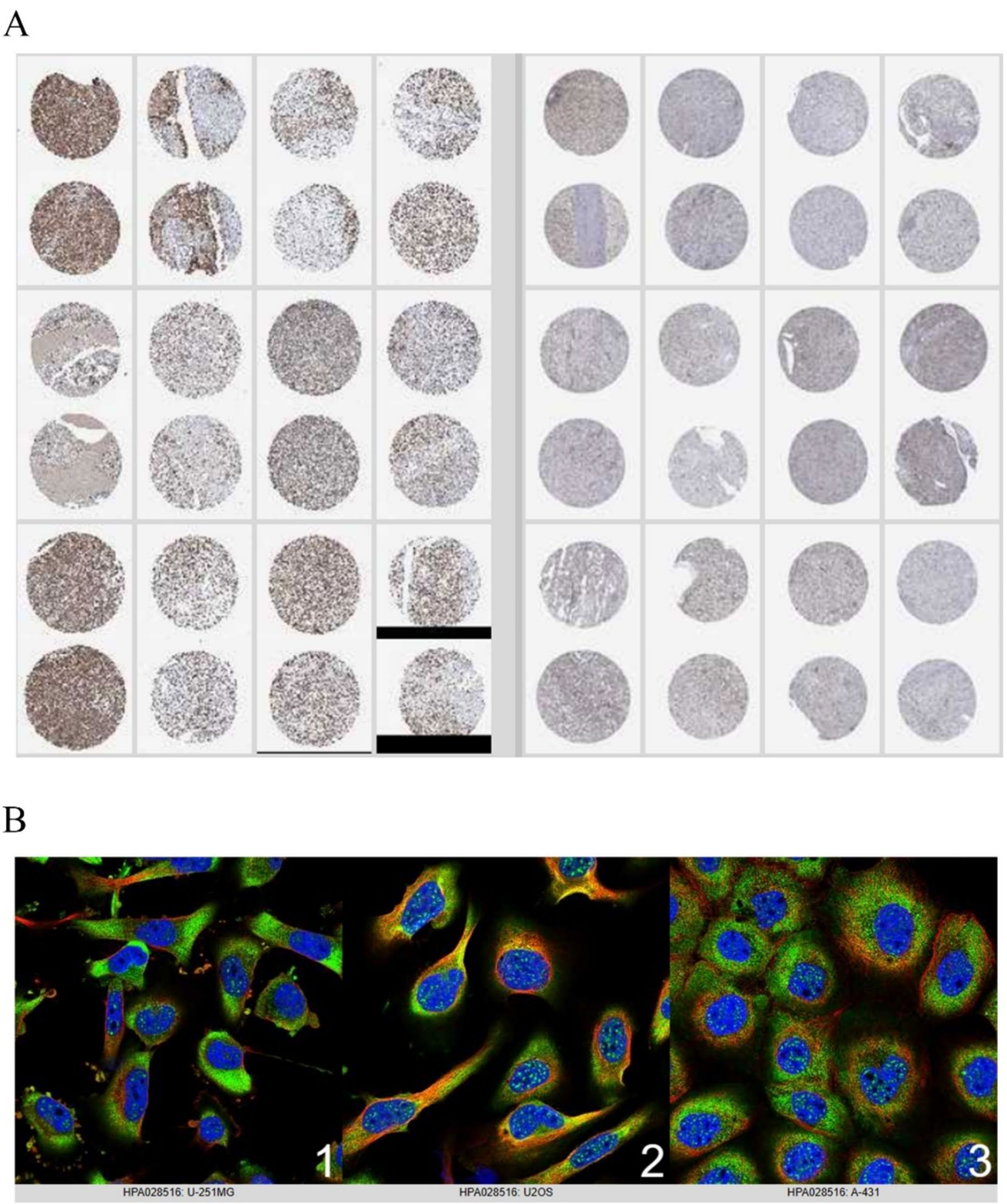

Fig. 2 Clarification of LIMK1 expression in ccRCC tissues. (**A**) The IHC images of LIMK1 in ccRCC tissues showed strong staining intensity of LIMK1. (**B**) Immunofluorescence images for the distribution of LIMK1 protein in three cell lines (U-251MG, U2OS, and A-431). LIMK1 was predominantly observed in the cytosol and slightly seen in nuclear speckles

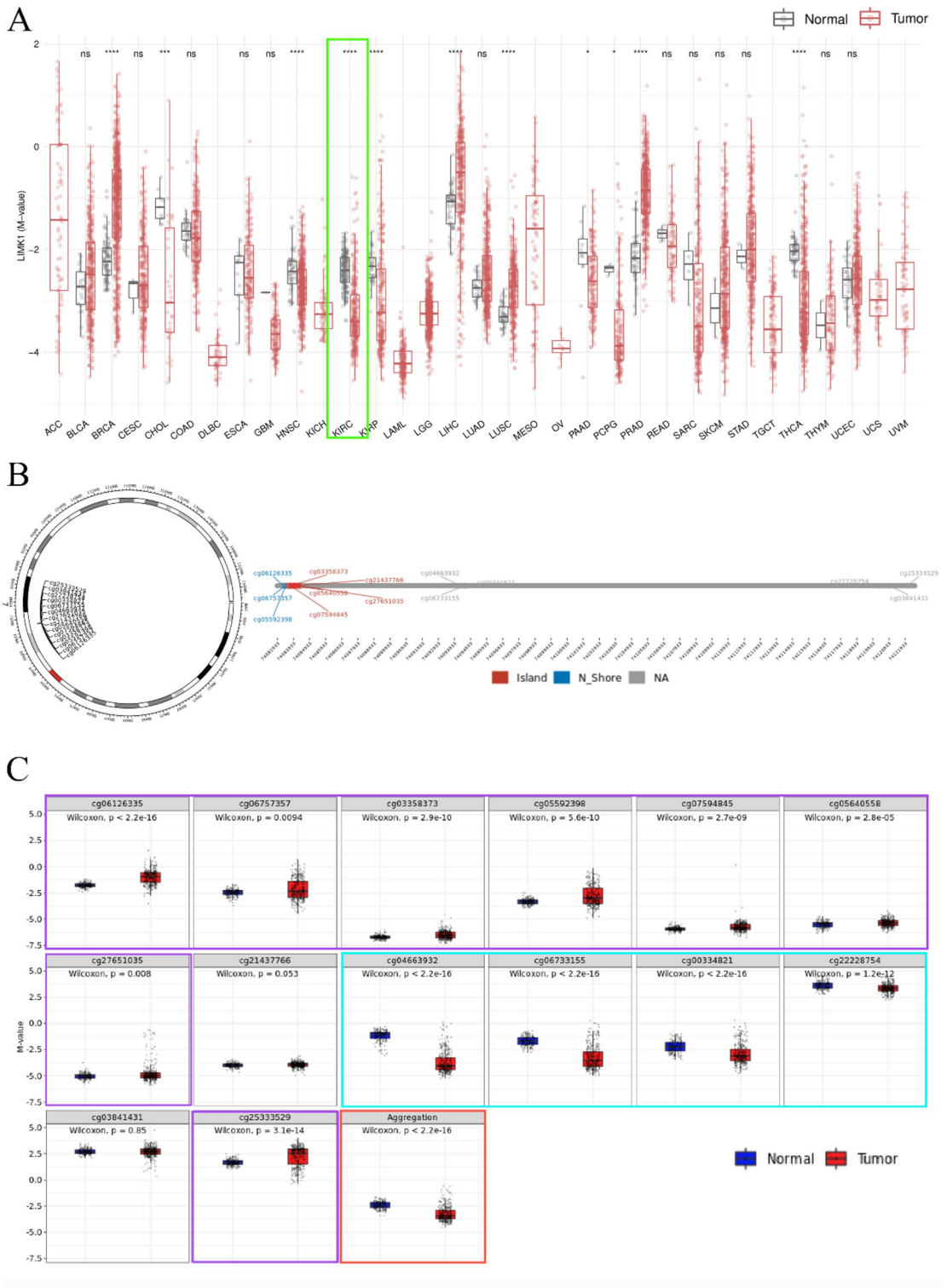

Fig. 3 DNA methylation of LIMK1 in patients with ccRCC. (**A**) The differential expression of LIMK1 methylation examined in tumor and normal samples in pan-cancer. (**B**) The location of 14 LIMK1 methylation probes in chromosome 12, specifically within CpG Island. Five probes are situated within the Island region (cg07594845, cg05640558, cg03358373, cg21437766, cg27651035), three probes are located in the N_Shore region (cg05592398, cg06126335, cg06757357), and six probes (cg22228754, cg03841431, cg25333521, cg00334821, cg06733155, cg04663932) are situated in gene body region. (**C**) The methylation status of each LIMK1 probe and its aggregation level. The purple box means elevated methylation levels. The blue box means decreased methylation levels. The red box means the aggregation methylation levels. *$p<0.05$, ***$p<0.001$, ****$p<0.0001$, n.s. $p>0.05$

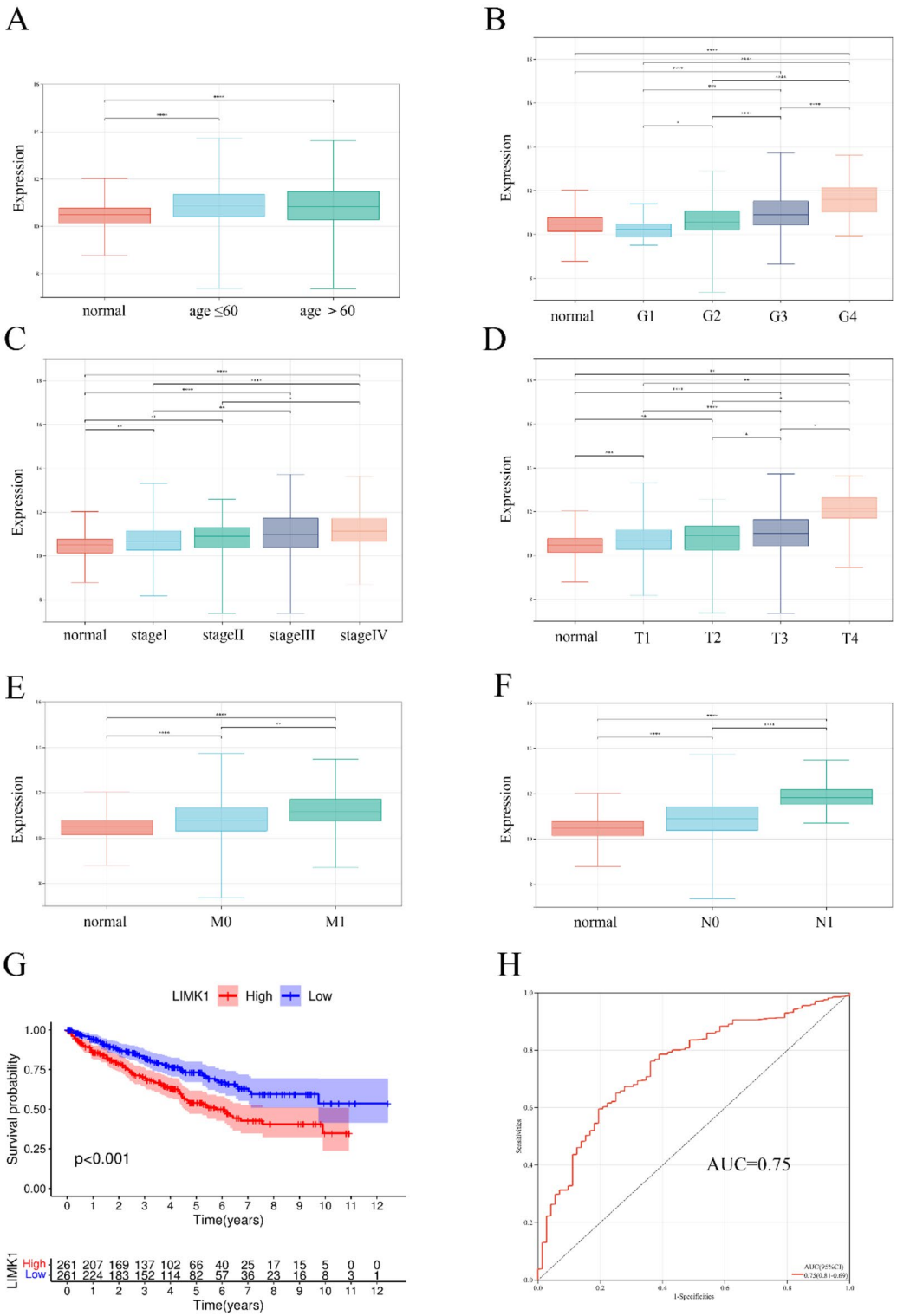

Fig. 4 LIMK1 expression was associated with the clinicopathologic parameters. (**A**–**F**) LIMK1 expression in patients with ccRCC with different clinicopathological features (age, histological grade, pathological stage, and TNM scores) using the TCGA-ccRCC cohort. (**G**) Kaplan-Meier survival analysis between high- and low-LIMK1 expression groups. (**H**) The ROC curve representing the diagnostic value of LIMK1 expression in ccRCC. *$p<0.05$, **$p<0.01$, ***$p<0.001$, ****$p<0.0001$, n.s. $p>0.05$

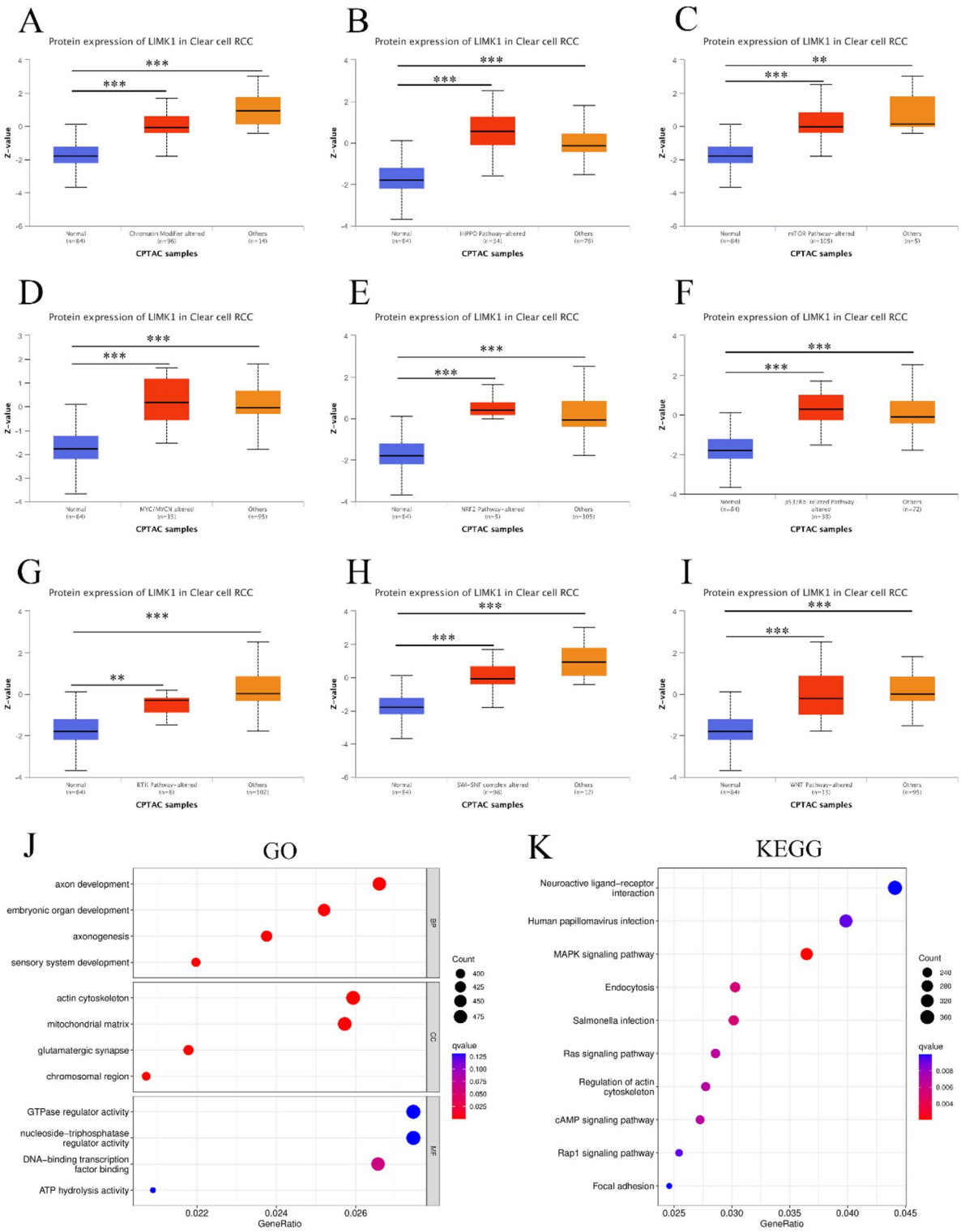

Fig. 5 Involvement of signaling pathways and functional enrichment. (**A–I**) Multiple pathways are involved, including chromatin modifier alteration, Hippo, mTOR, MYC/MYCN, NRF2, p53/Rb, RTK, SWI-SNF complex, and WNT. The dataset comprises 110 cases obtained from CPTAC-ccRCC. Mass spectrometry was used to quantify the LIMK1 protein level. The Z-values indicate the standard deviations from the median across samples for the specific cancer type. (**J**) GO and (**K**) KEGG analyses based on DEGs. $^{**}p<0.01$, $^{***}p<0.001$

The interaction of LIMK1 expression with the immune system

Next, the relationship between LIMK1 and immune system was assessed. Figure 6A depicted the negative correlations between LIMK1 expression and two well-known TSGs (APC and PTEN), which have been reported to inhibit the development of ccRCC (Whiteside 2006; Maekawa et al. 1999). Increasing studies have shown that the infiltration of immune cells plays an important role in the development of cancer (Kang et al. 2021). Figure 6B demonstrated a negative correlation between LIMK1 expression and clinical outcomes of patients with ccRCC. Meanwhile, the high levels of $CD4^+$ T cells and macrophages indicated better survival time. There was a positive correlation between LIMK1 expression and immune cell types, including B cells, $CD4^+$ T cells, macrophages, neutrophils, and DCs (Fig. 6C). Together, these findings suggest a significant association between LIMK1 expression and immune cells in patients with ccRCC.

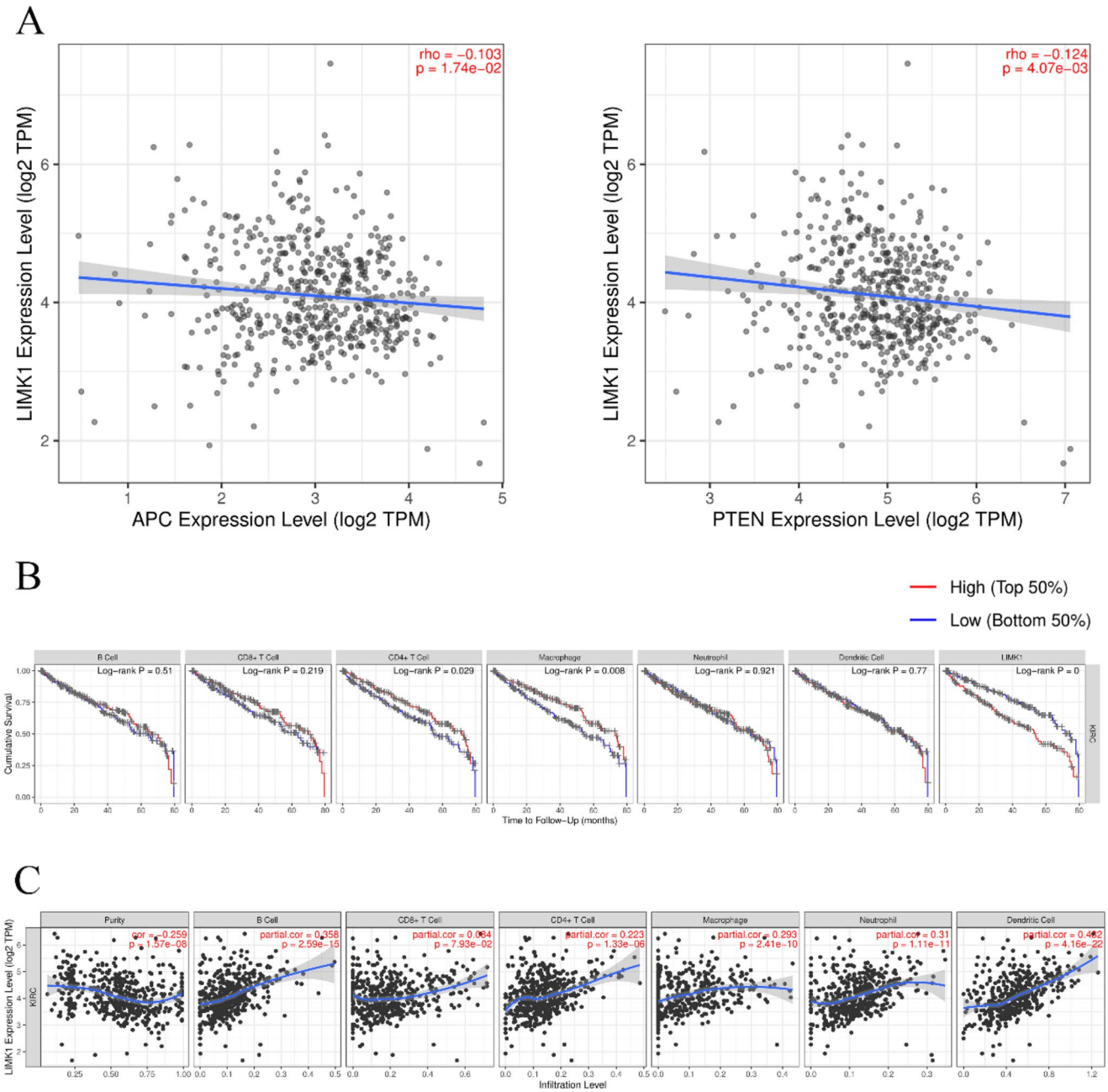

Fig. 6 The interaction of LIMK1 expression with the immune system. (**A**) Analysis of LIMK1 and tumor suppressor genes (APC and PTEN). (**B**) The relevance between clinical outcome and LIMK1 expression as well as six immune cells (B cells, $CD8^+$ T cells, $CD4^+$ T cells, macrophages, neutrophils, and dendritic cells) in patients with ccRCC. (**C**) The correlation between LIMK1 expression and different immune cells

Correlation of LIMK1 expression and immune checkpoint genes

Immune-checkpoint molecules are crucial for tumor cells evading the immune surveillance (Whiteside 2006). Whether LIMK1 is correlated with immune checkpoint genes was explored. As illustrated in Fig. 7A, there were positive correlations between LIMK1 expression and CD274, CTLA4, HAVCR2, LAG3, PDCD1, and PDCD1LG2 in patients with ccRCC. Figure 7B displayed the scatter plot of the correlation between LIMK1 expression and individual genes. TIDE scores of the high-LIMK1 group were higher than those of the low-LIMK1 group, indicating that patients with high-LIMK1 are more likely to escape the immune surveillance and less likely to respond to immune therapy (Fig. 7C). Taken together, the aforementioned analyses suggest that increased LIMK1 expression may act as an indicator of patients with enhanced immune evasion.

Investigation of biological function of LIMK1 in vitro

To determine the biological role of LIMK1 in RCC, LIMK1 was silenced in RCC. Western blotting was used to verify the knockdown efficiency, and si-LIMK1#2 was chosen for the subsequent experiments due to its effective knockdown performance (Fig. 8A). The CCK-8 assay illustrated that the silencing of LIMK1 decreased the proliferation of A-498 cells (Fig. 8B). The transwell assay revealed that LIMK1 knockdown resulted in a decrease in the number of migrated and invasive A-498 cells, respectively (Fig. 8C and D). For 786-0 cells, after knockdown of LIMK1, the reduction of proliferation, migration, and invasion ability of 786-0 cells was examined via colony assay (Figure S7A), wound healing assay (Figure S7B), and transwell assay (Figure S7C), respectively. The findings suggest that LIMK1 contributes to the proliferation, migration, and invasion of RCC cells in vitro. Recently, LIMK1 has been shown to phosphorylate and deactivate ADF/cofilin, leading to a stabilization of the actin cytoskeleton (Maekawa et al. 1999; Kang et al. 2021). Thus, we examined whether the absence of LIMK1 prevents the phosphorylation of cofilin in ccRCC. In A-498 cells, the elimination of LIMK1 caused dephosphorylation of cofilin (Fig. 8E). Our findings demonstrate that the inhibition of LIMK1 leads to a decrease in the phosphorylation of cofilin in RCC cells, thus potentially diminishing their migration and invasion capabilities.

Relevance of LIMK1 and drug sensitivity

Considering the limited effectiveness of chemotherapy drugs for ccRCC, it is imperative to explore better and innovative drugs for treatment. The correlation between LIMK1 expression and drug sensitivity was analyzed. The analysis showed that high LIMK1 was associated with increased drug sensitivity to several medications, including Bleomycin, Simvastatin, Everolimus, Staurosporine, Rapamycin, and Wortmannin (Fig. 9). All of these drugs in tumor treatment are currently commonly used. In sum, these results broaden the scope of therapeutic options available for patients.

Discussion

ccRCC is a malignant cancer, known for its low sensitivity to radiotherapy and chemotherapy (Zynda et al. 2016). LIMK1 has been reported to be involved in the development of cancers, especially in cell migration (Kang et al. 2021; Qiao et al. 2021). However, the role of LIMK1 in ccRCC remains unclear. In this study, we first investigated the expression level and prognosis value of LIMK1 in ccRCC. Clearly, ccRCC patients with high LIMK1 expression were associated with poor prognosis in TCGA-ccRCC and FAHWMU cohorts. Additionally, LIMK1 was related to immune infiltration, immune checkpoints, and drug sensitivity in ccRCC. Furthermore, the impacts of LIMK1 inhibition on the proliferation, migration, and invasion of RCC cells was examined in A-498 and 786-0 cell lines. Our findings suggest that LIMK1 may serve as a novel biomarker for ccRCC.

Utilizing the TCGA and CPTAC databases, increased LIMK1 expression was identified at transcription level and protein level in ccRCC. Consistently, the high expression of LIMK1 expression was confirmed in four RCC cell lines (ACHN, A-498, 786-0, and caki-1) and tumor tissues from FAHWMU cohort. DNA methylation, as a key epigenetic mechanism, is involved in the development of RCC (Shenoy et al. 2015). Herein, our research unveiled the DNA methylation level of specific sites of LIMK1 was associated with the survival probability of patients with ccRCC. Recently, immune checkpoints have been reported to be involved in tumor immune surveillance and immune evasion (Deng and Zhang 2018). In this study, it has been demonstrated that LIMK1 was positively correlated with immune checkpoint-related genes, such as CD274 and LAG3. Exploration of immune treatment response indicated that patients with high LIMK1 expression had poorer response to immunotherapy. The efficacy of immune checkpoint inhibitors (ICIs) could be evaluated using TIDE scores (Fu et al. 2020; Jiang et al. 2018). However, the efficacy of ICIs is not solely contingent upon the expression levels of immune checkpoints. Other crucial factors, for example, the tumor microenvironment, also influence the efficacy of ICIs (Pitt et al. 2016). Therefore, assessing the role of ICIs in ccRCC patients requires

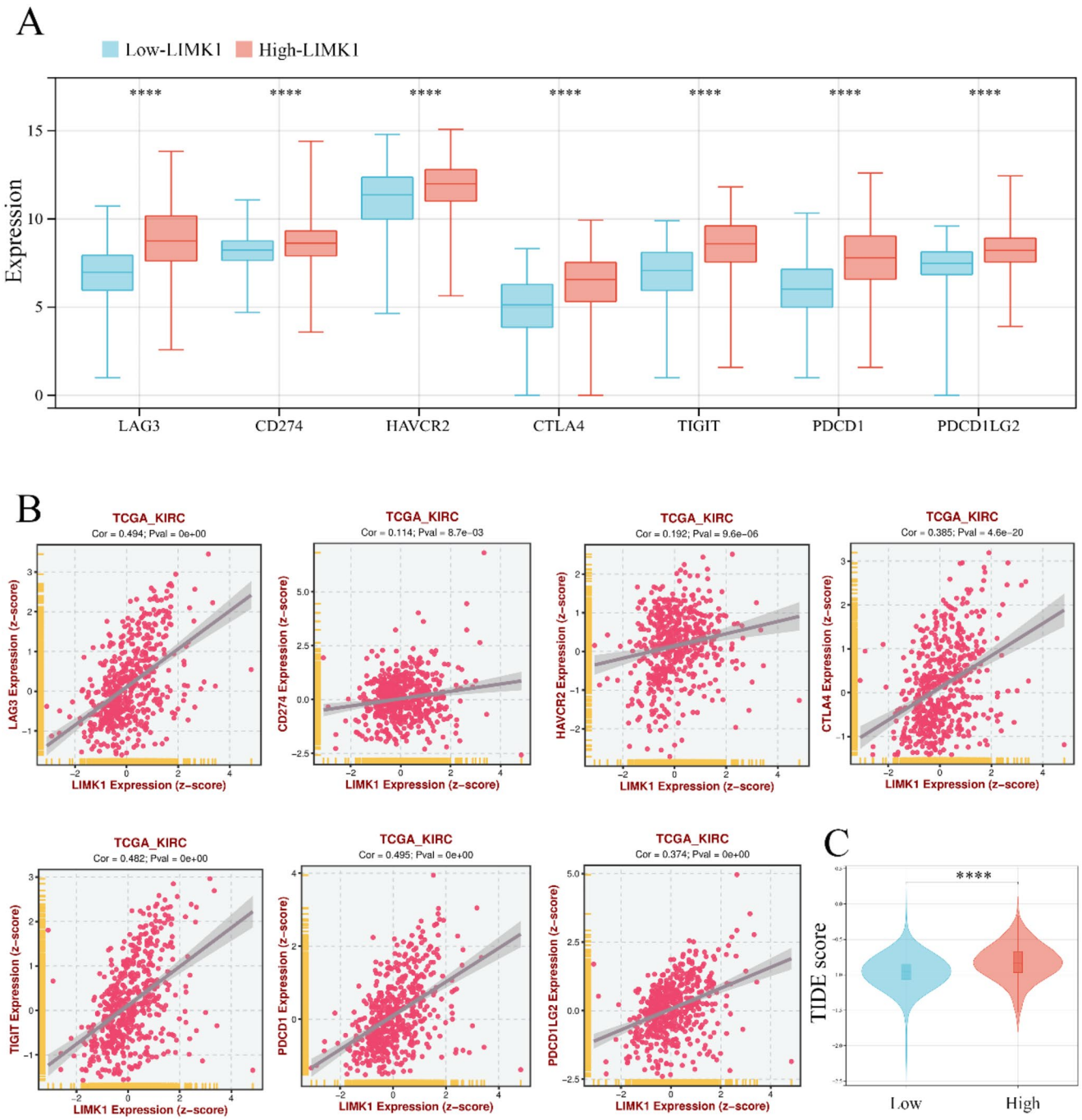

Fig. 7 Correlation of LIMK1 expression and immune checkpoint genes. (**A**) Correlation between LIMK1 and immune checkpoint genes was analyzed based on the TCGA-ccRCC cohort. (**B**) Correlation of LIMK1 expression and individual immune checkpoint genes. (**C**) TIDE scores in the high- and low-LIMK1 expression groups using the TCGA-ccRCC cohort. ****$p < 0.0001$

larger number of ccRCC patients to elucidate the underlying mechanisms.

LIMK1 was found to be significantly enriched in multiple cancer-promoting pathways (Hippo, mTOR, MYC/MYCN, RTK, SWI-SNF complex, WNT, p53/Rb, and NRF2) (Marignol et al. 2013; Wang et al. 2023; Korkut et al. 2018; Xu et al. 2023; Zhou et al. 2020; Shaw et al. 2019). Insightfully, the development of RCC is strongly influenced by inflammation (Liu et al. 2018). We found that there was a correlation between LIMK1 expression and the NRF2 pathway, which is known to be involved in inflammation (Saha et al. 2020). These findings suggest that LIMK1 may play a role in the pathogenic mechanisms of ccRCC through interacting with these pathways.

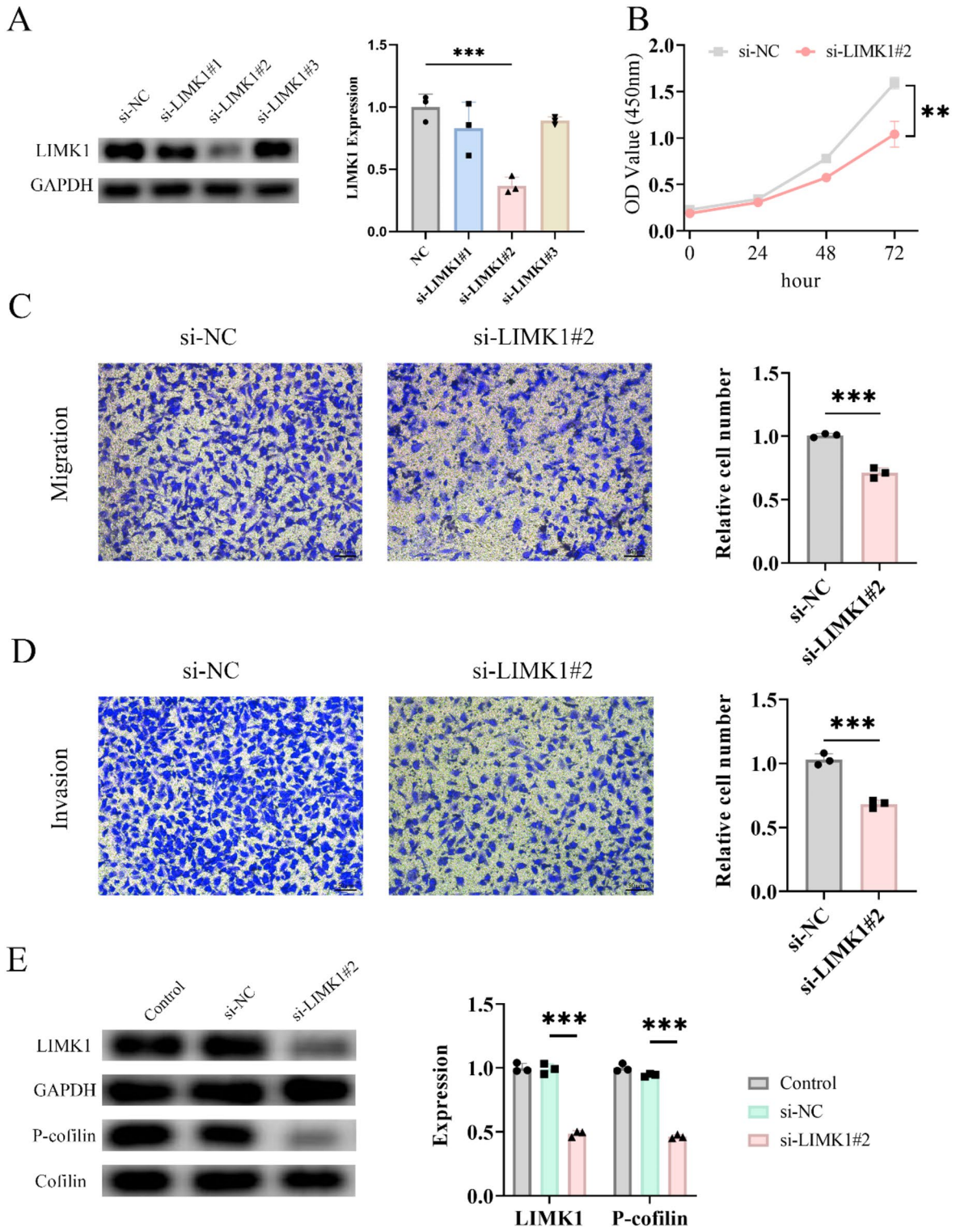

Fig. 8 Investigation of biological function of LIMK1 in vitro. (**A**) LIMK1 protein level. (**B**) Cell proliferation in the A-498 cell line. (**C** and **D**) Migration and invasion. (**E**) LIMK1 knockdown decreased p-cofilin level in A-498 cells. $^{**}p<0.01$, $^{***}p<0.001$

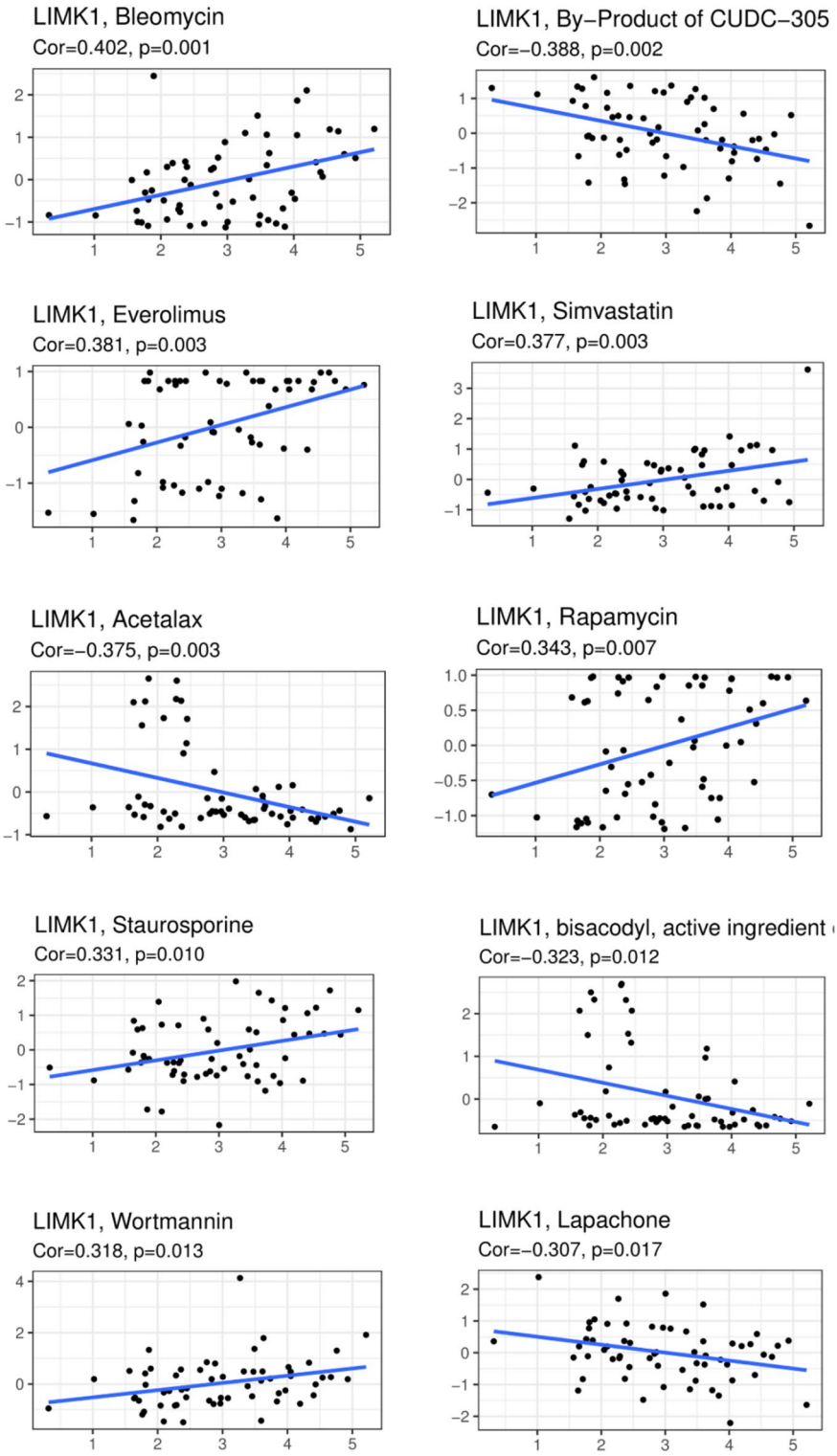

Fig. 9 Relevance of LIMK1 and drug sensitivity. Correlation between LIMK1 and drug sensitivity

There is a consensus that the landscape of immune cell infiltration in tumor microenvironments is intricate (Liu et al. 2019). Our findings showed that LIMK1 was associated with immune cells, such as T cells, B cells, neutrophils, macrophages, and DCs. Previous studies have shown that infiltration of subtypes of $CD4^+$ T cell, tumor-associated macrophages, neutrophils and DC cells correlates with poor prognosis in RCC (Toma et al. 2015; Wang et al. 2018; Song et al. 2015; Santoni et al. 2013). Combined with these, LIMK1 may promote the progression of ccRCC by regulating the immune cells infiltration. The mutation of BAP1 has been reported to

be correlated with the progression of RCC (Bi et al. 2016; Joseph et al. 2016). Herein, it was found that LIMK1 was correlated with the mutation of BAP1, suggesting that the involvement of LIMK1 in ccRCC development may be associated with BAP1 mutation.

Next, the in vitro experiments confirmed that the knockdown of LIMK1 attenuated the proliferation, invasion, and migration ability of A-498 cells and 786-0 cells. It has been reported that cofilin, a downstream effector of LIMK1, is essential in controlling actin dynamics, which is associated with tumor migration, invasion, and metastasis (Tanouchi et al. 2016; Mohan et al. 2019; Davidson and Wood 2016; Bernard 2007; Lee et al. 2017). Our findings revealed that when LIMK1 was silenced, cofilin phosphorylation was inhibited. Collectively, the above findings suggest that the LIMK1-cofilin pathway may be the underlying mechanism of LIMK1 in promoting ccRCC cell migration and invasion. As the pharmaceutical industry advances, there is a growing emphasis on predicting drug sensitivity through public database. Drug sensitivity analysis showed that LIMK1 expression was linked to drug sensitivity of many medications, including Bleomycin, Simvastatin, Everolimus, Staurosporine, Rapamycin and Wortmannin, expanding options for personalized drug selection for ccRCC patients. Nevertheless, the precise molecular mechanisms of LIMK1 regulating tumor progression require more experimental validation in vivo and in vitro.

Conclusions

In summary, LIMK1 is identified as a novel promoter of ccRCC and holds promising predictive potential for the prognosis of ccRCC.

Supplementary Information The online version contains supplementary material available at https://doi.org/10.1007/s00432-025-06146-5 .

Acknowledgements We sincerely appreciate the TCGA, UCSC Xena, CPTAC, THPA, SMART software, MethSurv database, TIMER databases, UALCAN platform, and CellMiner database that are freely available to us. Some elements in the graphical abstract were created using Figdraw (authorization code: SWSIA26828).

Author contributions Yifei Li and Siqi Wang designed the study. Yifei Li collected the data, and conducted the experiments; Congcong Fan, Feng Jiang, and Jingnan Zhang performed the statistical analysis; Yanzhen Li, Rui Zhang and Zhixian Yu drafted of the manuscript; Yifei Li, Congcong Fan, and Yanjie Jiang revised the manuscript; Siqi Wang revised the work. All authors read and approved the submitted version.

Funding This research did not receive any specific grant from funding agencies in the public, commercial, or not-for-profit sectors.

Data availability The data that support the findings of this study are available from the corresponding author upon reasonable request.

Declarations

Ethics approval and consent to participate The studies involving human participants were reviewed and approved by the Ethics Committees of the First Affiliated Hospital of Wenzhou Medical University (KY2023-263). The patients/participants provided their written informed consent to participate in this study.

Consent for publication Not applicable.

Competing interests The authors declare no competing interests.

References

Bénédetti H, Vallée B (2023) LIM kinases: from molecular to pathological features. Cells. 12(12)

Bernard O (2007) Lim kinases, regulators of actin dynamics. Int J Biochem Cell Biol 39(6):1071–1076

Bi M, Zhao S, Said JW, Merino MJ, Adeniran AJ, Xie Z et al (2016) Genomic characterization of sarcomatoid transformation in clear cell renal cell carcinoma. Proc Natl Acad Sci U S A 113(8):2170–2175

Cohen HT, McGovern FJ (2005) Renal-cell carcinoma. N Engl J Med 353(23):2477–2490

Davidson AJ, Wood W (2016) Unravelling the actin cytoskeleton: A new competitive edge?? Trends Cell Biol 26(8):569–576

Deng H, Zhang Z (2018) The application of nanotechnology in immune checkpoint Blockade for cancer treatment. J Control Release 290:28–45

Fu J, Yu J, Chen J, Xu H, Luo Y, Lu H (2018) In vitro inhibitory properties of sesquiterpenes from Chloranthus serratus on cell motility via down-regulation of LIMK1 activation in human breast cancer. Phytomedicine 49:23–31

Fu J, Li K, Zhang W, Wan C, Zhang J, Jiang P et al (2020) Large-scale public data reuse to model immunotherapy response and resistance. Genome Med 12(1):21

Gong H, Zhou L, Khelfat L, Qiu G, Wang Y, Mao K et al (2019) Rho-Associated protein kinase (ROCK) promotes proliferation and migration of PC-3 and DU145 prostate Cancer cells by targeting LIM kinase 1 (LIMK1) and matrix Metalloproteinase-2 (MMP-2). Med Sci Monit 25:3090–3099

Hammers H (2016) Immunotherapy in kidney cancer: the past, present, and future. Curr Opin Urol 26(6):543–547

Hsieh JJ, Purdue MP, Signoretti S, Swanton C, Albiges L, Schmidinger M et al (2017) Renal cell carcinoma. Nat Rev Dis Primers 3:17009

Jemal A, Bray F, Center MM, Ferlay J, Ward E, Forman D (2011) Global cancer statistics. CA Cancer J Clin 61(2):69–90

Jiang P, Gu S, Pan D, Fu J, Sahu A, Hu X et al (2018) Signatures of T cell dysfunction and exclusion predict cancer immunotherapy response. Nat Med 24(10):1550–1558

Jonasch E, Walker CL, Rathmell WK (2021) Clear cell renal cell carcinoma ontogeny and mechanisms of lethality. Nat Rev Nephrol 17(4):245–261

Joseph RW, Kapur P, Serie DJ, Parasramka M, Ho TH, Cheville JC et al (2016) Clear cell renal cell carcinoma subtypes identified by BAP1 and PBRM1 expression. J Urol 195(1):180–187

Kang X, Li W, Liu W, Liang H, Deng J, Wong CC et al (2021) LIMK1 promotes peritoneal metastasis of gastric cancer and is a therapeutic target. Oncogene 40(19):3422–3433

Korkut A, Zaidi S, Kanchi RS, Rao S, Gough NR, Schultz A et al (2018) A Pan-Cancer analysis reveals High-Frequency genetic alterations in mediators of signaling by the TGF-β superfamily. Cell Syst 7(4):422–37e7

Lee SY, Kim W, Lee YG, Kang HJ, Lee SH, Park SY et al (2017) Identification of sennoside A as a novel inhibitor of the slingshot (SSH) family proteins related to cancer metastasis. Pharmacol Res 119:422–430

Li Y, Ge D, Lu C (2019) The SMART app: an interactive web application for comprehensive DNA methylation analysis and visualization. Epigenetics Chromatin 12(1):71

Liu XY, Zhang FR, Shang JY, Liu YY, Lv XF, Yuan JN et al (2018) Renal Inhibition of miR-181a ameliorates 5-fluorouracil-induced mesangial cell apoptosis and nephrotoxicity. Cell Death Dis 9(6):610

Liu X, Xu J, Zhang B, Liu J, Liang C, Meng Q et al (2019) The reciprocal regulation between host tissue and immune cells in pancreatic ductal adenocarcinoma: new insights and therapeutic implications. Mol Cancer 18(1):184

Ljungberg B, Bensalah K, Canfield S, Dabestani S, Hofmann F, Hora M et al (2015) EAU guidelines on renal cell carcinoma: 2014 update. Eur Urol 67(5):913–924

Maekawa M, Ishizaki T, Boku S, Watanabe N, Fujita A, Iwamatsu A et al (1999) Signaling from Rho to the actin cytoskeleton through protein kinases ROCK and LIM-kinase. Science 285(5429):895–898

Marignol L, Rivera-Figueroa K, Lynch T, Hollywood D (2013) Hypoxia, Notch signalling, and prostate cancer. Nat Rev Urol 10(7):405–413

McConnell BV, Koto K, Gutierrez-Hartmann A (2011) Nuclear and cytoplasmic LIMK1 enhances human breast cancer progression. Mol Cancer 10:75

Mertins P, Tang LC, Krug K, Clark DJ, Gritsenko MA, Chen L et al (2018) Reproducible workflow for multiplexed deep-scale proteome and phosphoproteome analysis of tumor tissues by liquid chromatography-mass spectrometry. Nat Protoc 13(7):1632–1661

Moch H, Cubilla AL, Humphrey PA, Reuter VE, Ulbright TM (2016) The 2016 WHO classification of tumours of the urinary system and male genital Organs-Part A: renal, penile, and testicular tumours. Eur Urol 70(1):93–105

Mohan AS, Dean KM, Isogai T, Kasitinon SY, Murali VS, Roudot P et al (2019) Enhanced dendritic actin network formation in extended lamellipodia drives proliferation in Growth-Challenged Rac1(P29S) melanoma cells. Dev Cell 49(3):444–60e9

Pavlović N, Heindryckx F (2021) Exploring the role of Endoplasmic reticulum stress in hepatocellular carcinoma through mining of the human protein atlas. Biology (Basel). 10(7)

Pitt JM, Marabelle A, Eggermont A, Soria JC, Kroemer G, Zitvogel L (2016) Targeting the tumor microenvironment: removing obstruction to anticancer immune responses and immunotherapy. Ann Oncol 27(8):1482–1492

Qiao Y, Jin T, Guan S, Cheng S, Wen S, Zeng H et al (2021) Long noncoding RNA Lnc-408 promotes invasion and metastasis of breast cancer cell by regulating LIMK1. Oncogene 40(24):4198–4213

Saha S, Buttari B, Panieri E, Profumo E, Saso L (2020) An overview of Nrf2 signaling pathway and its role in inflammation. Molecules. 25(22)

Santoni M, Massari F, Amantini C, Nabissi M, Maines F, Burattini L et al (2013) Emerging role of tumor-associated macrophages as therapeutic targets in patients with metastatic renal cell carcinoma. Cancer Immunol Immunother 62(12):1757–1768

Scott RW, Olson MF (2007) LIM kinases: function, regulation and association with human disease. J Mol Med (Berl) 85(6):555–568

Shaw B, Burrell CL, Green D, Navarro-Martinez A, Scott D, Daroszewska A et al (2019) Molecular insights into an ancient form of Paget's disease of bone. Proc Natl Acad Sci U S A 116(21):10463–10472

Shenoy N, Vallumsetla N, Zou Y, Galeas JN, Shrivastava M, Hu C et al (2015) Role of DNA methylation in renal cell carcinoma. J Hematol Oncol 8:88

Song W, Li L, He D, Xie H, Chen J, Yeh CR et al (2015) Infiltrating neutrophils promote renal cell carcinoma (RCC) proliferation via modulating androgen receptor (AR) → c-Myc signals. Cancer Lett 368(1):71–78

Sung H, Ferlay J, Siegel RL, Laversanne M, Soerjomataram I, Jemal A et al (2021) Global Cancer statistics 2020: GLOBOCAN estimates of incidence and mortality worldwide for 36 cancers in 185 countries. CA Cancer J Clin 71(3):209–249

Tanouchi A, Taniuchi K, Furihata M, Naganuma S, Dabanaka K, Kimura M et al (2016) CCDC88A, a prognostic factor for human pancreatic cancers, promotes the motility and invasiveness of pancreatic cancer cells. J Exp Clin Cancer Res 35(1):190

Toma M, Wehner R, Kloß A, Hübner L, Fodelianaki G, Erdmann K et al (2015) Accumulation of tolerogenic human 6-sulfo LacNAc dendritic cells in renal cell carcinoma is associated with poor prognosis. Oncoimmunology 4(6):e1008342

Villalonga E, Mosrin C, Normand T, Girardin C, Serrano A, Žunar B et al (2023) LIM kinases, LIMK1 and LIMK2, are crucial node actors of the cell fate: molecular to pathological features. Cells. 12(5)

Wang Y, Wang Y, Xu L, Lu X, Fu D, Su J et al (2018) CD4+T cells promote renal cell carcinoma proliferation via modulating YBX1. Exp Cell Res 363(1):95–101

Wang YQ, Wu DH, Wei D, Shen JY, Huang ZW, Liang XY et al (2023) TEAD4 is a master regulator of high-risk nasopharyngeal carcinoma. Sci Adv 9(1):eadd0960

Whiteside TL (2006) Immune suppression in cancer: effects on immune cells, mechanisms and future therapeutic intervention. Semin Cancer Biol 16(1):3–15

Xu L, Pierce JL, Sanchez A, Chen KS, Shukla AA, Fustino NJ et al (2023) Integrated genomic analysis reveals aberrations in WNT signaling in germ cell tumors of childhood and adolescence. Nat Commun 14(1):2636

Yu Y, Wang Z, Zheng Q, Li J (2021) FAM72 serves as a biomarker of poor prognosis in human lung adenocarcinoma. Aging 13(6):8155–8176

Zhang Y, Li A, Shi J, Fang Y, Gu C, Cai J et al (2018) Imbalanced LIMK1 and LIMK2 expression leads to human colorectal cancer progression and metastasis via promoting β-catenin nuclear translocation. Cell Death Dis 9(7):749

Zhang W, Zhang Q, Zhu C, Shi Z, Shao C, Chen Y et al (2022) The intrarenal landscape of T cell receptor repertoire in clear cell renal cell cancer. J Transl Med 20(1):558

Zhou Y, Wang K, Zhou Y, Li T, Yang M, Wang R et al (2020) HEATR1 deficiency promotes pancreatic cancer proliferation and gemcitabine resistance by up-regulating Nrf2 signaling. Redox Biol 29:101390

Zhou F, Zeng L, Chen X, Zhou F, Zhang Z, Yuan Y et al (2022) DUSP10 upregulation is a poor prognosticator and promotes cell proliferation and migration in glioma. Front Oncol 12:1050756

Zynda ER, Schott B, Babagana M, Gruener S, Wernher E, Nguyen GD et al (2016) An RNA interference screen identifies new avenues for nephroprotection. Cell Death Differ 23(4):608–615